Published OnlineFirst January 30, 2013; DOI: 10.1158/1541-7786.MCR-12-0456

Molecular Cancer Research

Inhibition of *TWIST1* Leads to Activation of Oncogene-Induced Senescence in Oncogene-Driven Non –Small Cell Lung Cancer

Timothy F. Burns, Irina Dobromilskaya, Sara C. Murphy, et al.

Mol Cancer Res 2013;11:329-338. Published OnlineFirst January 30, 2013.

Published OnlineFirst January 30, 2013; DOI: 10.1158/1541-7786.MCR-12-0456

Cell Cycle and Senescence

Molecular Cancer Research

Inhibition of *TWIST1* Leads to Activation of Oncogene-Induced Senescence in Oncogene-Driven Non–Small Cell Lung Cancer

Timothy F. Burns[1], Irina Dobromilskaya[1], Sara C. Murphy[1], Rajendra P. Gajula[2], Saravanan Thiyagarajan[2], Sarah N.H. Chatley[4], Khaled Aziz[2], Yoon-Jae Cho[3], Phuoc T. Tran[1,2], and Charles M. Rudin[1]

Abstract

A large fraction of non–small cell lung cancers (NSCLC) are dependent on defined oncogenic driver mutations. Although targeted agents exist for *EGFR*- and *EML4-ALK*–driven NSCLCs, no therapies target the most frequently found driver mutation, *KRAS*. Furthermore, acquired resistance to the currently targetable driver mutations is nearly universally observed. Clearly a novel therapeutic approach is needed to target oncogene-driven NSCLCs. We recently showed that the basic helix-loop-helix transcription factor *Twist1* cooperates with mutant *Kras* to induce lung adenocarcinoma in transgenic mouse models and that inhibition of Twist1 in these models led to *Kras*-induced senescence. In the current study, we examine the role of *TWIST1* in oncogene-driven human NSCLCs. Silencing of *TWIST1* in *KRAS*-mutant human NSCLC cell lines resulted in dramatic growth inhibition and either activation of a latent oncogene-induced senescence program or, in some cases, apoptosis. Similar effects were observed in *EGFR* mutation–driven and *c-Met*–amplified NSCLC cell lines. Growth inhibition by silencing of *TWIST1* was independent of p53 or p16 mutational status and did not require previously defined mediators of senescence, p21 and p27, nor could this phenotype be rescued by overexpression of *SKP2*. In xenograft models, silencing of *TWIST1* resulted in significant growth inhibition of *KRAS*-mutant, *EGFR*-mutant, and *c-Met*–amplified NSCLCs. Remarkably, inducible silencing of *TWIST1* resulted in significant growth inhibition of established *KRAS*-mutant tumors. Together these findings suggest that silencing of *TWIST1* in oncogene driver–dependent NSCLCs represents a novel and promising therapeutic strategy. *Mol Cancer Res; 11(4); 329–38. ©2013 AACR.*

Introduction

Lung cancer is the leading cause of cancer death in the United States and worldwide. The 5-year survival rate for all patients with lung cancer is a dismal 15% (1). The recent advances in the treatment of non–small cell lung cancers (NSCLC) have come from recognition that NSCLCs that is not a single disease entity but rather a collection of distinct molecularly driven neoplasms. This paradigm is typified by the recent progress made in the treatment of patients with *EGFR*-mutant and *EML4-ALK* translocation–driven adenocarcinomas of the lung with tyrosine kinase inhibitors targeting these oncogenes (2). Unfortunately, acquired resistance to the currently targetable driver mutations arises in nearly all cases, typically within the first 2 years of therapy (3, 4). Furthermore, little if any progress has been made in the treatment of patients with the most frequently observed driver oncogene, mutant *KRAS*. It has been over 2 decades since the first mutation in the *KRAS* oncogene was identified in NSCLCs. *KRAS* is mutated in one third of all malignancies and approximately 20% of all NSCLCs (5). *KRAS* mutation, which results in a constitutively active oncoprotein, has been shown to predict lack of benefit from chemotherapy in the adjuvant setting, to portend worse prognosis in metastatic NSCLCs, and possibly to increase risk of recurrence in early-stage disease (5). Although testing for *KRAS* mutation status is routinely done, there are no currently approved therapies targeting this critical pathway in NSCLCs.

The principle of "oncogene addiction," the absolute dependency on an oncogene for a tumor's survival, has been

Authors' Affiliations: Departments of [1]Oncology and [2]Radiation Oncology & Molecular Radiation Sciences, The Sidney Kimmel Comprehensive Cancer Center at the Johns Hopkins University School of Medicine, Baltimore, Maryland; [3]Department of Neurology and Neurosurgery, Stanford University School of Medicine and Lucile Packard Children's Hospital, Stanford, California; and [4]Department of Medicine, Division of Hematology-Oncology, Hillman Cancer Center, University of Pittsburgh, Pittsburgh, Pennsylvania

Note: Supplementary data for this article are available at Molecular Cancer Research Online (http://mcr.aacrjournals.org/).

Current address for T.F. Burns: Department of Medicine, Division of Hematology-Oncology, Hillman Cancer Center, University of Pittsburgh, Pittsburgh, PA.

Corresponding Author: Charles M. Rudin, Sidney Kimmel Comprehensive Cancer Center at Johns Hopkins University, David H. Koch Cancer Research Building, Room 544, 1550 Orleans Street, Baltimore MD 21231. Phone: 410-502-0678; Fax: 410-502-0677; E-mail: rudin@jhmi.edu

doi: 10.1158/1541-7786.MCR-12-0456

Published OnlineFirst January 30, 2013; DOI: 10.1158/1541-7786.MCR-12-0456

well-supported by several preclinical models and in multiple tumor types (6). An emerging concept of "non-oncogene addiction," the dependency of tumor cells on factors which are not inherently oncogenic, but which are required for survival due to the oncogenic state of the tumor, is now gaining acceptance. To that end, several investigators have conducted large-scale synthetic lethal screens looking for genes,. which are essential for survival of *KRAS*-mutant tumor cells and have suggested therapeutic strategies that may specifically target *KRAS*-mutant tumors (7–11). To date, it is unclear whether the inhibition of candidate genes identified in these screens can reproducibly produce synthetic lethality in *KRAS*-mutant cancer specifically or are more generally required for tumor proliferation (12).

Another potential therapeutic strategy in *KRAS*-mutant tumors is activation of latent oncogene–induced senescence (OIS). OIS is an irreversible cell-cycle arrest that is characterized by cells displaying an enlarged, flattened cytoplasm, increased senescence-associated β-galactosidase (SA-β-Gal) activity, increased chromatin condensation and changes in gene expression associated with DNA damage and cell-cycle checkpoint pathways. OIS is thought to be triggered early during tumorigenesis after oncogene activation and serves as a checkpoint to prevent premalignant lesions from progressing to malignancy (13).

The emerging concept of using prosenescence therapies for cancer has generated considerable interest (14, 15). Interestingly, several studies have shown that bypass of senescence in mouse models of mutant *Kras*–mediated adenocarcinoma of the lung and pancreas is essential for tumorigenesis (16–18). Therefore, activation of OIS in *KRAS*-mutant NSCLCs may be an effective therapeutic strategy. Disruption of the p53–ARF and p16–Rb pathways was previously thought to be required for bypass of RAS-mediated senescence (18). However, recent data suggest that the requirement of these pathways is context-dependent, as inactivation of Skp2 can lead to activation of OIS independent of the p53–ARF pathway through Atf4, p27, and p21 (19). Activation of suppressed senescence pathways in *KRAS*-mutant NSCLCs through inhibition of key downstream mediators of OIS would be a valuable treatment in NSCLCs.

Previous murine studies have suggested a role for Twist1 as a factor in preventing OIS through inhibition of the Rb and p53 pathways (20, 21). TWIST1 is a basic helix-loop-helix (bHLH) transcription factor which plays critical roles throughout development influencing mesoderm formation, neurogenesis, myogenesis, and neural crest cell migration and differentiation (22). These roles are highlighted by the findings that *Twist1* deletion is embryonic lethal in mice and that germ line haploinsufficiency of *TWIST1* in humans leads to Saethre–Chotzen syndrome, which is characterized by craniosynostosis and limb abnormalities (23, 24). A number of reports have implicated TWIST1 in oncogenesis through its ability to inhibit DNA damage–induced apoptosis, prevent OIS and promote metastasis through induction of the epithelial–mesenchymal transition (EMT; ref. 25). Increased *TWIST1* expression is correlated with increased risk of metastasis and poor prognosis in a number of solid tumor types including breast, prostate, ovarian, and lung (25). We have recently shown that *Twist1* cooperates with mutant *Kras* to induce adenocarcinoma of the lung in transgenic mouse models and inhibition of *Twist1* in these models led to activation of *Kras*-induced senescence (26). However, significant differences exist between transgenic mouse models of cancer and human disease. In the current study, we explore whether *TWIST1* plays a critical role in human NSCLCs characterized by multiple defined oncogenic drivers.

Materials and Methods

Cell culture

All human NSCLC cell lines, (A549, H460, H358, H727, H23, Calu-1, Calu-6, H1975, H3255, H1993) and embryonic kidney cell line HEK 293T were obtained from the American Type Culture Collection and grown in media as recommended.

SA-β-gal staining

At 12 ± 2 days after infection with short hairpin RNA (shRNA) lentiviruses, the cells were washed twice with PBS and then fixed with PBS containing 2% formaldehyde and 0.25% glutaraldehyde for 5 minutes. The cells were then incubated at 37ºC for 20 hours with staining solution [40 mmol/L citric acid sodium phosphate, pH 6.0, 1 mg/mL 5-bromo-4-chloro-3-isolyl-b-D-galactoside (X-gal), 5 mmol/L potassium ferricyanide, 5 mmol/L potassium ferrocyanide, 150 mmol/L NaCl, 2 mmol/L $MgCl_2$]. After incubation, cells were washed twice with PBS and viewed with bright-field microscopy.

Immunoblot analysis

Cells were lysed on ice for 60 minutes in radioimmunoprecipitation assay buffer supplemented with protease and phosphatase inhibitors (Sigma-Aldrich) and clarified by centrifugation. Protein concentrations were determined by Bradford protein assay (Bio-Rad Laboratories). Equal protein concentrations of each sample were run on NuPAGE bis-Tris gels (Invitrogen) and electrophoretically transferred to polyvinylidene difluoride membranes. After being blocked with 5% dried milk in TBS containing 0.2% Tween 20, the filters were incubated with primary antibodies. The following primary antibodies were used: goat anti-Actin (C-11, Santa Cruz), rabbit anti-GAPDH (FL-335, Santa Cruz), anti-p21 (Ab-1, Calbiochem), mouse monoclonal anti-p27 (F-8, Santa Cruz), rabbit anti-Parp-1/2 (H-250, Santa Cruz) rabbit anti-cleaved PARP (Cell Signaling), and anti-p53 (DO-1, Santa Cruz). After washing and incubation with horseradish peroxidase (HRP)-conjugated anti-goat or anti-mouse IgG (Amersham), the antigen–antibody complexes were visualized by chemiluminescence (ECL detection system; Perkin Elmer or SuperSignal West Femto Maximum Sensitivity Substrate; Thermo Fisher Scientific).

Colony formation assay

On days 4 or 6 after infection with the indicated shRNA lentiviruses, cells were plated in 12-well plates at a density of

Published OnlineFirst January 30, 2013; DOI: 10.1158/1541-7786.MCR-12-0456

5,000 to 10,000 cells/well. On day 12, the cells were stained with crystal violet (0.5% in 95% ethanol).

Cell-cycle analysis

Cells were harvested at indicated times, fixed with 70% cold ethanol and stained with stained with propidium iodide, and analyzed by flow cytometry as previously described (27).

Lentiviral shRNA and cDNA overexpression experiments

293T cells were seeded (2.5×10^6 cells) in T25 flasks. Lentiviral particles were generated using a three-plasmid system and infected as per the TRC Library Production and Performance Protocols, RNAi Consortium, Broad Institute (28) shRNA constructs were obtained from the Broad RNAi Consortium and clone IDs as are follows: TWIST1: TRCN0000020539 (shTWIST1-1) and TRCN0000020543 (shTWIST1-2). P53: TRCN0000003756 (shp53-1) and TRCN0000010814 (sh53-2). The pLKO.1-shRNA scramble vector was obtained from Dr. David M. Sabatini through Addgene (Addgene plasmid 1864) as previously described (29). The Tet-pLKO-puro vector was from Dmitri Wiederschain through Addgene (Addgene plasmid 21915) as previously described (30). The pLKO.1–Neo vector was obtained from Sheila Stewart through Addgene (Addgene plasmid 13425), and oligonucleotides for TWIST1-1, TWIST1-2, and scrambled control were cloned into this vector and used to for experiments with shRNAs targeting p53. All constructs were sequence-verified. Twenty-four hours after infection, cells were treated with 1 μg/mL puromycin or 500 μg/mL G418 and passaged once 80% confluent.

Xenograft experiments

A total of 5×10^5 viable cells were resuspended in equal volumes of PBS and Matrigel and injected subcutaneously in adult homozygous NOD/SCID mice (Harlan Laboratories). For doxycycline-inducible cell line experiments, once the tumors reached $\geq$150 mm^3 (average, 14 days), the mice were given 5% dextrose either with or without 2 mg/mL doxycycline in the drinking water. Drinking water was replenished at least once a week. Statistical analyses were conducted for each xenograft separately. Initial tumor volume measurements are summarized using means, SDs, and ranges. Growth patterns were summarized graphically by plotting the mean and SD for each treatment group over time. A conditional *t* test is used to compare shTWIST1 tumors with the control (shScram). $P < 0.05$ is considered statistically significant.

Results

Silencing of *TWIST1* activates latent OIS in human NSCLCs

To explore the role of *TWIST1* in human NSCLCs, we used an shRNA strategy to silence *TWIST1* in NSCLC cell lines with distinct mutational backgrounds (*KRAS*-mutant, *EGFR*-mutant and *c-Met*–amplified; Supplementary Table S1). In our previous study and current study, we have shown that the shRNAs used in this report (shTWIST1-1 and shTWIST-2) are able to significantly suppress TWIST1 levels on both the transcript and protein level (ref. 26 and Supplementary Fig. S1A and SB). Upon silencing of *TWIST1* with 2 separate shRNAs compared with a control scrambled shRNA, we observed dramatic growth inhibition in colony formation assays for all 9 NSCLC cell lines examined (Fig. 1). To confirm that these effects were not due to off-target effects of the shRNAs used in this study, we stably overexpressed a mouse *Twist1* cDNA in A549 cells and showed that this overexpression rescued the A549 cells from the growth-inhibitory effects of silencing human *TWIST1* (ref. 26 and Supplementary Fig. S2). In addition to the 9 lines shown in Fig. 1, an additional *KRAS*-mutant NSCLC cell line, Calu-6 showed extensive apoptosis by day 4 after silencing and could not be plated for this assay. In all, we observed significant growth inhibition in 7 *KRAS*-mutant NSCLC cell lines, 2 cell lines which harbor an activating mutation in *EGFR* as well as in a cell line with *c-Met* amplification. Taken together, these data suggest that *TWIST1* may play a critical role in lung cancer tumorigenesis in the context of multiple driver mutations.

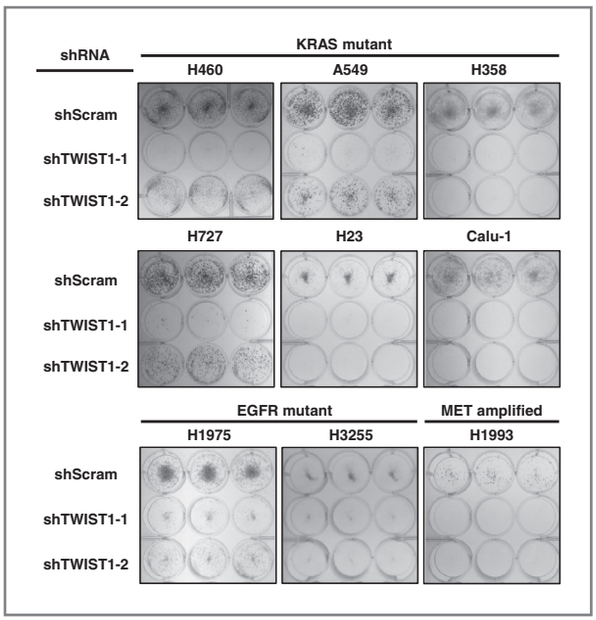

Figure 1. *TWIST1* knockdown results in growth inhibition in human NSCLCs. Silencing of *TWIST1* with 2 different shRNAs (shTWIST1-1 and shTWIST1-2) resulted in marked growth inhibition of *KRAS*-mutant (H460, A549, H358, H727, H23, and Calu-1), *EGFR*-mutant (H1975 and H3255), and a *c-Met*–amplified (H1993) NSCLC cell line, as shown by representative triplicates of crystal violet staining.

We observed a dramatic activation of latent OIS as shown by positive SA-β-Gal staining and characteristic enlarged, flattened cytoplasm morphology (Fig. 2) in 3 *KRAS*-mutant NSCLC cells lines (H460, A549, and H358). These findings were further supported by profound cell-cycle arrest in these cell lines (Fig. 3A) as well as by induction of the senescence markers, p21 and/or p27, in all cell lines examined (Fig. 3B).

Published OnlineFirst January 30, 2013; DOI: 10.1158/1541-7786.MCR-12-0456

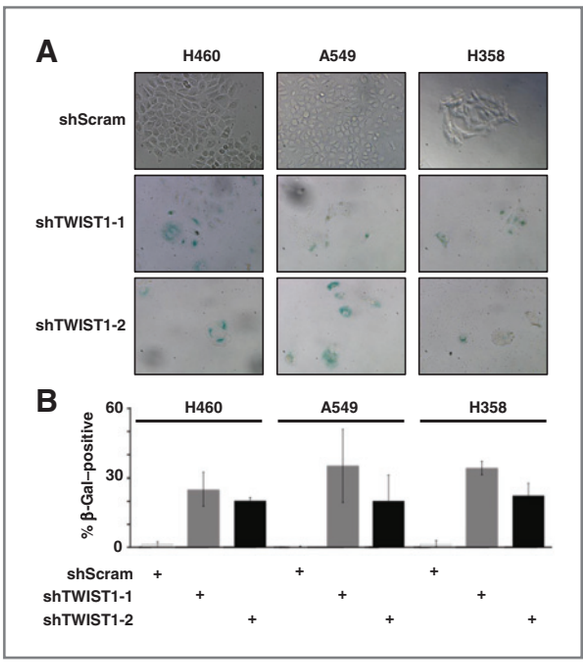

Figure 2. *TWIST1* knockdown activates latent OIS in human NSCLCs. A, representative photomicrographs (20×) of increased SA-β-gal staining in 3 representative NSCLC cell lines following shRNA-mediated *TWIST1* knockdown (above). B, quantification of SA-β-gal–stained cells following shRNA-mediated *TWIST1* knockdown.

Furthermore, a gene expression analysis after silencing of *TWIST1* in 3 *KRAS*-mutant cell lines (H460, H727, and H358) revealed several highly significant gene sets involved with growth arrest (Supplementary Figs. S7 and S8 and data not shown). Collectively, these series of experiments support a role for TWIST1 in the suppression of OIS in *KRAS*-mutant lung cancer cell lines. Interestingly, in a subset of cell lines (Calu-1, Calu-6), we also observed evidence of apoptosis including PARP cleavage. These findings are consistent with previously known antiapoptotic role of TWIST1 and suggest complementary mechanisms by which inhibition of TWIST1 may block tumor growth (31).

Growth inhibition by silencing *TWIST1* is not dependent on the p53/p21 pathway or p27/SKP2 pathway in NSCLC

A previous study had shown a requirement for p16 in mediating OIS in pancreatic ductal epithelial cells after silencing of *Twist1* (21). Furthermore, prior work had suggested a possible role for the p53/p21 pathway in mediating OIS after suppression of TWIST1 in human cancer cell lines (20). In the present study, we examined whether these pathways played a key role in mediating the growth inhibition observed after *TWIST1* silencing in human lung cancer cell lines. As the p16 pathway was disrupted either through deletion, methylation, or mutation in every cell line examined (Supplementary Table S1), it appeared that p16 was not required for the growth inhibition observed. In addition, only 2 (H460, A549) of the 10 lines had wild-type p53 which suggested that inhibition of p53 could not be the only mediator of growth inhibition after silencing of *TWIST1*. To test whether p53 was required for growth inhibition in p53 wild-type cell lines, we silenced p53 using an shRNA strategy and confirmed knockdown of p53 at baseline and under conditions that resulted in p53 stabilization (*TWIST1* knockdown and DNA damage; Fig. 4A, Supplementary Fig. S3 and data not shown). After knockdown of *TWIST1*, stabilization of p53 was observed in both the shScrambled control H460 and A549 cells and was accompanied by induction of p21. However, after silencing of p53, p53 expression and p21 induction were lost (Fig. 4A and Supplementary Fig. S3A). Despite the loss of p53 in these cell lines, growth inhibition induced by suppression of *TWIST1* was unaltered (Fig. 4B and Supplementary Fig. S3B). It is possible that through disabling a critical member of the OIS pathway such as p53, the cellular response after suppression of TWIST1 may shift from a senescence program to an apoptotic program. To assess whether a shift to an apoptotic program is occurring with depletion of p53, we have checked for evidence of PARP cleavage which is a well-validated marker of apoptosis. In H460 and A549 cells, we observed only a modest amount of apoptosis in our control shScram line after silencing of TWIST1. Interestingly, after depletion of p53, we observed a decrease in apoptosis compared with the control cells after silencing TWIST1 (Fig. 4). This would argue against apoptosis as significant mechanism for the observed growth inhibition as the modest decrease in apoptosis after p53 depletion did not result in even a partial rescue of the observed decrease in clonogenic survival following silencing of *TWIST1*.

As we had observed p53-independent p21 induction in several of our p53-disrupted cell lines (Fig. 3B), we examined whether p21 was required for the growth inhibition observed. We silenced p21 using shRNAs in 3 cell lines (H460, A549, and H727) and observed a significant reduction in p21 expression but not in the cyclin-dependent kinase inhibitor, p27 (Supplementary Fig. S4A). Silencing of p21 did not evidently affect the inhibition of colony formation induced by knockdown of *TWIST1* (Supplementary Fig. S4B).

Recent studies had suggested that the SKP2/p27 pathway was important for the induction of senescence (19). In addition, after silencing of *TWIST1*, we observed induction of p27 in several of these cell lines (Fig. 3B). We therefore attempted to knockdown p27 in H460 cells. Despite screening 8 shRNAs targeting p27, we were only able to derive a partial knockdown of this gene; complete knockdown prevented the establishment of a puromycin-resistant cell line even at early time points (Supplementary Fig. S5 and data not shown). It is possible that these cells lines require cytoplasmic p27, which has been shown in several studies to be oncogenic and can cooperate with *KRAS* in lung tumorigenesis (32) and reviewed in ref. 33). Partial knockdown of p27 markedly suppressed p27 induction after loss of *TWIST1*, however, growth inhibition was unperturbed (Supplementary Fig. S5B). To further evaluate the

Published OnlineFirst January 30, 2013; DOI: 10.1158/1541-7786.MCR-12-0456

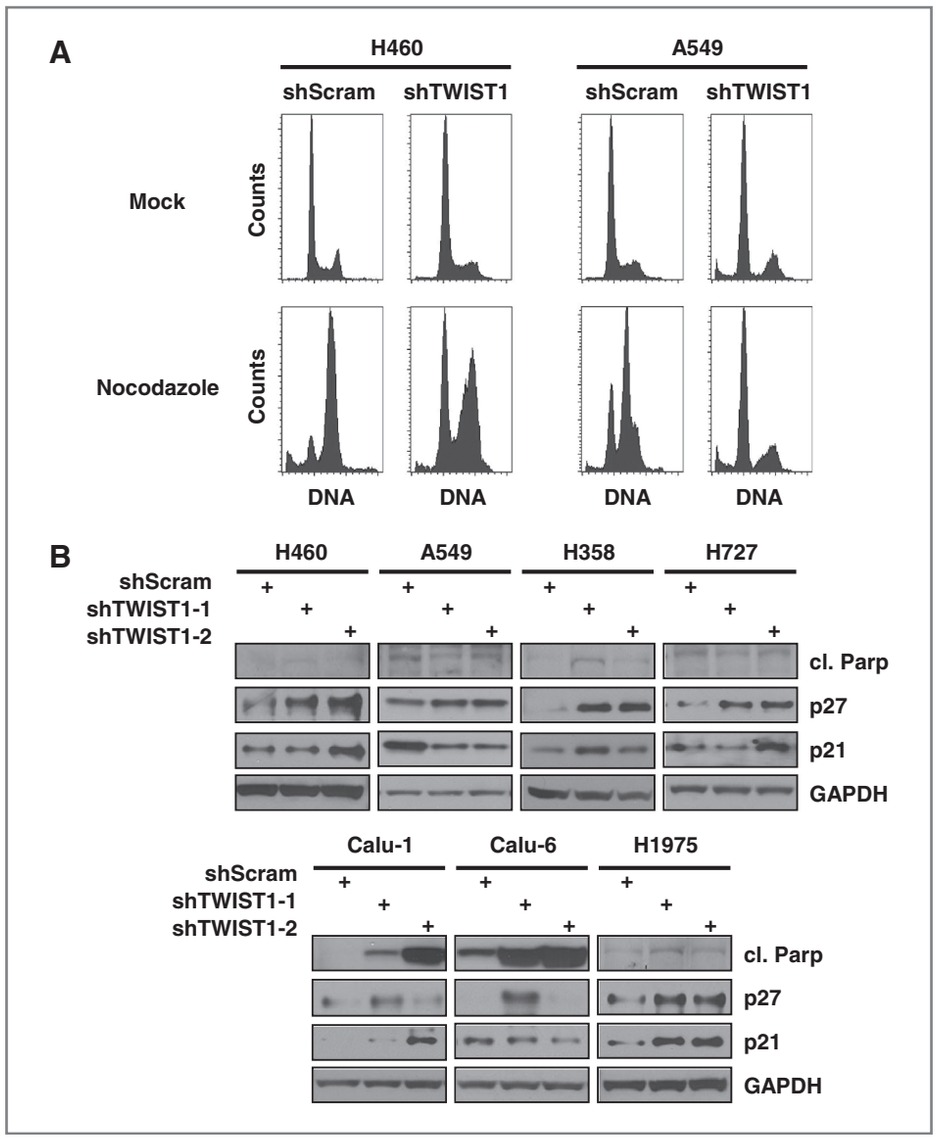

Figure 3. Inhibition of TWIST1 leads to a profound cell-cycle arrest and apoptosis in NSCLC cell lines. A, cell-cycle analysis with propidium iodide staining in H460 cells and A549 on days 8 and 6, respectively, after lentiviral shRNA infection. Bottom, mitotic trapping of cells with nocodazole (100 ng/mL) for 24 hours before harvesting. B, *TWIST1* knockdown in NSCLC cell lines results in the upregulation of markers of senescence, p21 and p27, as well as a marker of apoptosis, cleaved PARP, as shown by Western blotting on day 4 after infection.

requirement of the p27 pathway in mediating growth suppression after loss of *TWIST1*, we overexpressed the key regulator of p27 stability, *SKP2* (34) in the A549 and H460 cell lines. Overexpression of *SKP2* largely blocked p27 induction after silencing of *TWIST1* but did not rescue loss of *TWIST1* (Supplementary Fig. S6). Interestingly, loss of *TWIST1* expression in the setting of *SKP2* overexpression did result in modest increase in apoptosis as shown by the appearance of cleaved PARP.

Microarray analysis of NSCLC cell lines after silencing of *TWIST1* revealed a striking cell-cycle arrest gene signature

To further elucidate possible mechanisms of TWIST1 dependency in NSCLCs, we conducted microarray analysis on 3 *KRAS*-mutant NSCLC lung cancer cells (H460, H358, and H727) after silencing of *TWIST1*. A profound cell-cycle arrest signature was observed associated with silencing of *TWIST1* (Supplementary Fig. S7). Genes encoding general regulators of cell-cycle progression (cyclin D, E1, A2, B1, CDK2) and specific regulators of progression through S-phase (PCNA, SKP2) and mitosis (BUB1, CDC20, MAD2, AURKA, FOXM1) were significantly decreased after silencing of *TWIST1* (Supplementary Fig. S7). Gene set enrichment analysis (GSEA; ref. 35), comparing global gene expression patterns after *TWIST1* silencing with patterns from control (shScram) cell lines, revealed a highly significant similarity to multiple gene sets for cell-cycle arrest (Supplementary Fig. S8A). This dataset also showed highly significant similarity to a gene set predicting resistance to doxorubicin (Supplementary Fig. S8B). This is consistent with previous studies showing that *TWIST1* overexpression could confer chemoresistance in other tumor types (reviewed in ref. 25). Two gene sets involving the RAS signaling

Published OnlineFirst January 30, 2013; DOI: 10.1158/1541-7786.MCR-12-0456

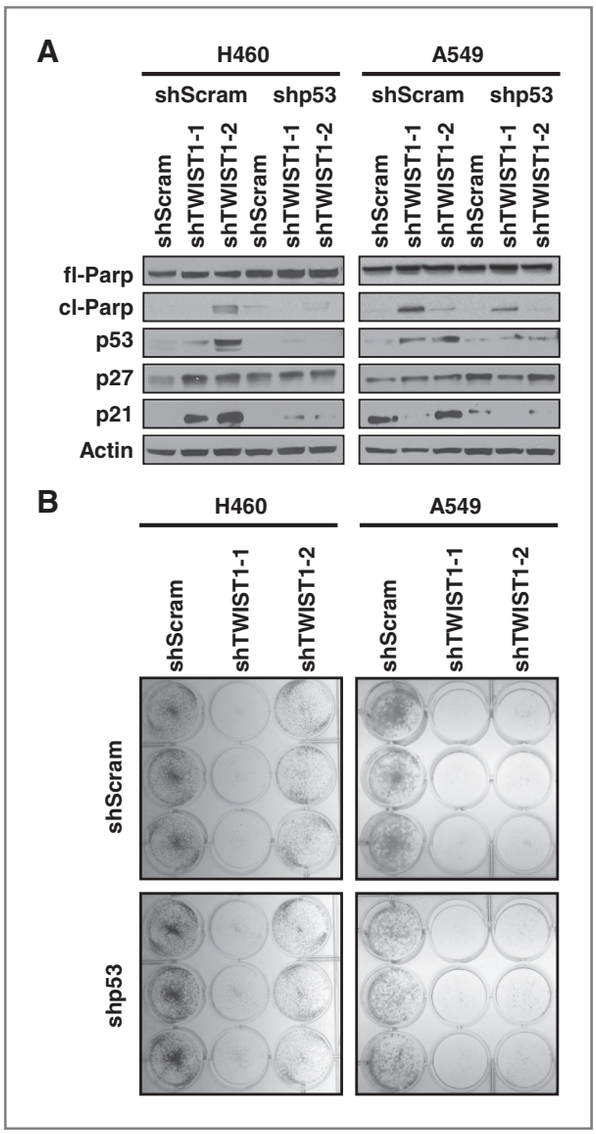

Figure 4. Growth inhibition by silencing *TWIST1* in NSCLCs is not p53-dependent. A, *TP53* knockdown in H460 and A549 cells prevents induction of p53 and its target gene, p21, after *TWIST1* knockdown as shown by Western blotting on days 12 and 6, respectively, after the shRNA infection. B, representative triplicates of crystal violet staining of H460 or A549 NSCLC cells show *TWIST1* knockdown with 2 separate shRNAs decreases cellular proliferation despite the absence of p53.

pathway were also highly significantly similar, including a gene signature of NRAS-induced genes (decreased in shTWIST1 compared with control), and a gene signature following exposure of cells to the RAS inhibitor, salirasib (Supplementary Fig. S8C). This is consistent with our findings that inhibition of TWIST1 is critical for *KRAS*-mutant NSCLC survival. Interestingly, a gene set for down-regulation of the target genes of YB-1, a known TWIST1 target gene (36), was also highly similar and suggests a possible role for YB-1 in mediating TWIST1 function (Supplementary Fig. S8D).

Silencing of *TWIST1* results in a significant growth inhibition in oncogene driver–dependent NSCLC xenograft models

To further evaluate TWIST1 as a potential therapeutic target for NSCLCs with a defined oncogenic driver, we examined the effect of TWIST1 targeting on both tumor initiation and maintenance in a xenograft hind flank model. *KRAS*-mutant (A549, H358, and H727), *EGFR*-mutant (H1975), and *c-Met*–amplified (H1993) NSCLC cell lines were infected with either scrambled shRNA or TWIST1-1 shRNA and on day 4 after infection were implanted in the hind flank of NOD/SCID animals. Knockdown of *TWIST1* significantly inhibited tumor growth in each of these oncogene-driven NSCLC xenograft models (Fig. 5). Remarkably, silencing of *TWIST1* in the *c-Met*–amplified and -dependent cell line H1993 completely prevented tumor formation, suggesting a potentially critical role for the TWIST1 pathway in this context.

To examine the role of TWIST1 in tumor maintenance of fully established tumors, we constructed syngeneic A549 cells containing either shRNA targeting *TWIST1* or a scrambled control under the control of a doxycycline-responsive promoter (30). In absence of doxycycline, these cell lines had similar growth characteristics. However, upon addition of doxycycline, *TWIST1* was silenced in the A549 Tet-shTWIST1 cell line, p21 was induced and growth inhibition was observed (Fig. 6A and B). To determine the requirement of *TWIST1* in established tumors, the A549 Tet-shScram and A549 Tet-shTWIST1 cell lines were implanted in the hind flank of NOD/SCID animals. After the formation of palpable tumors, doxycycline was added to the drinking water of half the animals for each tumor type. Although the administration of doxycycline to animals with A549 Tet-shScram xenograft tumors did not affect the growth kinetics, silencing of *TWIST1* by doxycycline administration to animals with the A549 Tet-shTWIST1 xenografts resulted in significant growth inhibition (Fig. 6C). Interestingly, this growth inhibition was accompanied by induction of p21 specifically in the tumors in which TWIST1 was silenced. This finding supports the role of growth arrest and OIS in mediating the observed growth inhibition *in vivo*. In summary, these data suggest that inhibition of *TWIST1* in established tumors may be an effective therapeutic strategy.

Discussion

We have shown that TWIST1 is a promising novel therapeutic target for oncogene-driven NSCLCs, through activation of OIS. We found that silencing of *TWIST1* resulted in dramatic growth inhibition and activation of latent OIS and/or apoptosis. This marked growth inhibition appeared to be independent of the p53/p21, p16, and SKP2/p27 pathways. Similar effects were seen in *KRAS*-mutant, *EGFR*-mutant, and *c-MET*–amplified cell lines, suggesting that inhibition of TWIST1 may be a potential therapeutic target in a large percentage of patients with oncogene-driven lung cancer.

Published OnlineFirst January 30, 2013; DOI: 10.1158/1541-7786.MCR-12-0456

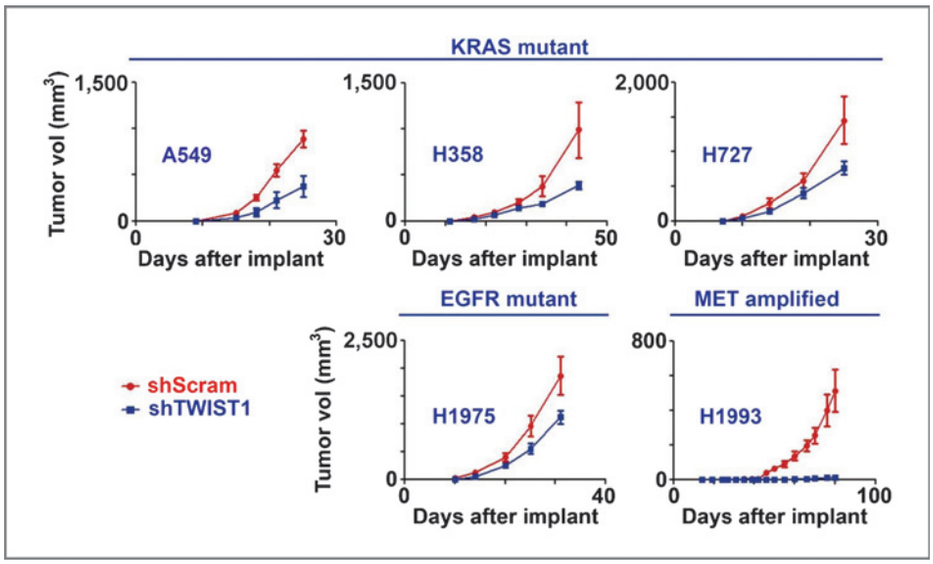

Figure 5. Silencing of *TWIST1* results in a significant growth inhibition in oncogene-dependent NSCLC xenograft models. Representative studies in which *KRAS*-mutant (A549, H358 and H727), *EGFR*-mutant (H1975), and *c-Met*–amplified (H1993) NSCLC cell lines were infected with shRNA targeting *TWIST1* (blue filled squares) or scrambled control (shScram; red closed circles), respectively, and on day 4 after infection, equal numbers of viable cells were injected in the hind flank of NOD/SCID animals and allowed to establish palpable tumors. Once established tumors formed, tumor volumes were measured every 3 days for the duration of the experiment ($P < 0.05$ for all models).

Although it has been more than 2 decades since the first mutation in the *KRAS* oncogene was identified in NSCLCs, no current therapies target this critical oncogene. In this study, we have shown that TWIST1 is required for proliferative growth of oncogene-driven NSCLCs including multiple *KRAS*-mutant lines and that silencing of *TWIST1* leads

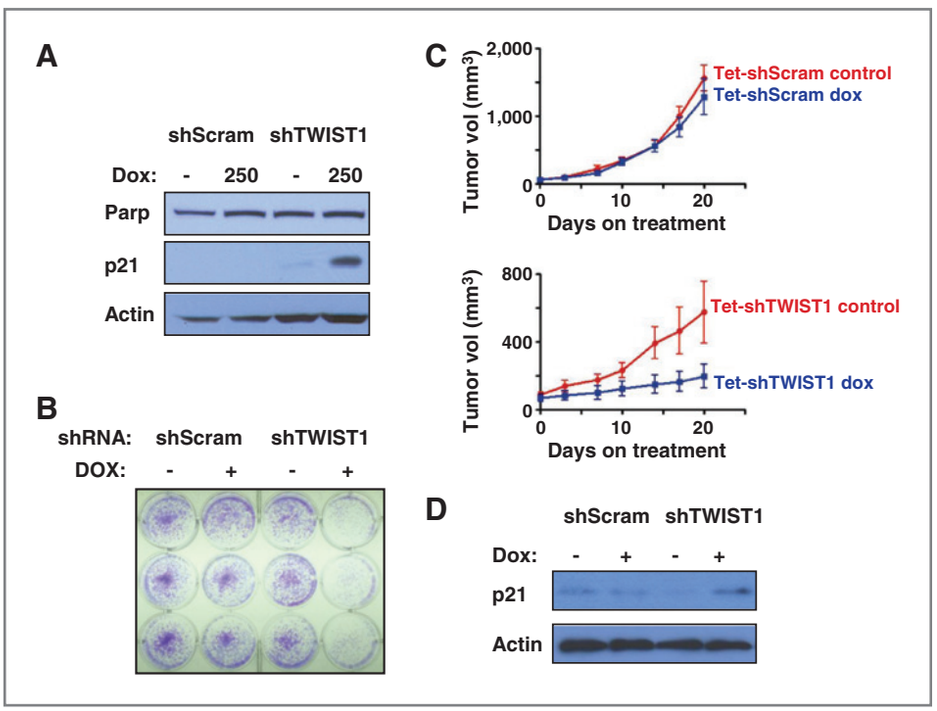

Figure 6. Inducible silencing of *TWIST1* results in a significant growth inhibition of established NSCLC tumors. A, induction of the doxycycline-inducible shRNA targeting *TWIST1* after addition of doxycycline (250 ng/mL) to the media results in p21 induction as shown by Western blotting on day 8 after treatment. B, representative triplicates of crystal violet staining in A549 cells carrying doxycycline-inducible shRNAs targeting scrambled control or *TWIST1* respectively. C, A549 cells carrying a doxycycline-inducible shRNA targeting scrambled control (Tet-shScram) or *TWIST1* (Tet-shTWIST1), respectively, were injected in the hind flank of NOD/SCID animals and allowed to establish palpable tumors. Once established tumors formed, at least 6 animals in each group were given 5% dextrose with (blue filled squares) or without (red closed circles) 2 mg/mL doxycycline in the drinking water, and tumor volumes were measured every 3 days for the duration of the experiment ($P < 0.05$ for Tet-shTWIST1; NS for shScram). D, induction of p21 in xenograft tumors containing A549 Tet-shTWIST1 in the presence of doxycycline. Tumors were harvested at 21 days after the initiation of 5% dextrose with or without 2 mg/mL doxycycline in the drinking water. Western blot analysis was conducted for p21 and β-actin.

Published OnlineFirst January 30, 2013; DOI: 10.1158/1541-7786.MCR-12-0456

to activation of OIS. Previous studies have defined the bypass of senescence as a requirement for mutant *KRAS*-mediated carcinogenesis in the lung (16–18). In this current study, we elucidated a possible synthetic interaction between mutant *KRAS* and *TWIST1* that in most lines results not in lethality but in the activation of latent OIS. Our findings are consistent with a recent study of KRAS transformation of primary pancreatic duct epithelial cells that showed activated mutant *KRAS* led to increased expression of TWIST1 by a posttranscriptional mechanism and that TWIST1 expression was essential to bypassing OIS in this model (21) We have recently shown that *Twist1* overexpression cooperates with mutant *Kras* to induce adenocarcinoma of the lung in mouse models, and inhibition of *Twist1* in these models led to activation of *Kras*-induced senescence (26). One possible caveat to this mouse model study was that simultaneous expression of $Kras^{G12D}$ and *Twist1* during tumorigenesis could have resulted in co-dependent tumors and therefore the phenotype of tumor stasis and activation of OIS observed with removal of *Twist1* overexpression was due to this induced co-dependency. However, our current work shows the *TWIST1* dependency of oncogene-driven NSCLCs generally and *KRAS*-mutant NSCLCs in particular using both *in vitro* and xenograft approaches.

Previous work had suggested that bypass of OIS by TWIST1 required p16 and possibly a functional p53/p21 pathway (20, 21). In our multiple lung cancer lines, we observed activation of OIS in both p53 wild-type and mutant backgrounds and in the absence of a functional p16 pathway. Furthermore, our knockdown experiments confirmed that the observed OIS and growth inhibition was p53/p21-independent. A recent study has shown a critical role of TWIST1 in sarcomagenesis through its ability to lead to p53 degradation (37), and previous studies have shown the ability of TWIST1 to interact with and influence the transcriptional function of p53 (38, 39). Furthermore, p53 is required for Ras-induced OIS in mouse embryonic fibroblasts (18). Although the dispensability of p53 for OIS after silencing of TWIST1 was unexpected, it is consistent with the previous work that first established the role of TWIST1 in suppressing OIS (20). Ansieau and colleagues observed induction of p21 and p16 after silencing of TWIST1 and subsequently proposed a role for the p53 and Rb pathways in mediating OIS after suppression of TWIST1. However, in the same study, they clearly showed the induction of OIS after silencing of TWIST1 or TWIST2 in 2 p53-mutant cell lines (T47D and RPMI 7951; ref. 20). The aforementioned study about the role of TWIST1 in sarcoma showed a requirement for p53 in mediating serum starvation senescence after silencing of TWIST1 in a single sarcoma cell line (37). It is not clear whether the requirement for p53 is a sarcoma-specific effect or is required under conditions of serum starvation. Our current study suggests that both the p53 and p16 pathways are dispensable for OIS and growth inhibition observed after suppression of TWIST1.

In addition, using both knockdown of p27 and overexpression of SKP2, we have also shown that activation of OIS is likely independent of the SKP2/p27 pathway. An important caveat is that in neither experiment were we able to completely deplete p27 from the cell and it remains possible that this is a p27-dependent process requiring only a low threshold expression of p27. Alternatively, p21 and p27 may be redundant and knockdown of both CDK inhibitors is required for abrogation of OIS induced by silencing of *TWIST1*. Furthermore, in our experiments using SKP2 overexpression cell lines, we did observe an increase in apoptosis in the SKP2-overexpressing lines compared with vector control. Therefore, we cannot rule out the possibility that the ability of SKP2 overexpression to rescue the OIS phenotype was masked, in part, by the increase in apoptosis that was observed. However, for all experiments, in which we have silenced TWIST1, we have assessed the cells for SA-β-gal staining and have not seen a rescue of OIS after depletion or overexpression of any genes in this study.

Despite these caveats, these data suggest that alternative p53/p21- and SKP2/p27-independent mechanisms may exist for the activation of OIS. A recent study suggested that the endoplasmic reticulum (ER) stress protein and transcription factor ATF4 was important for p53-independent OIS induced by Skp2 inhibition (19). In addition, there are some data suggesting that unopposed expression of oncogenes such as β-catenin can result in DNA damage resulting in senescence and apoptosis independent of p53 (40). To better characterize the mediators of TWIST dependency, we are conducting overexpression and loss of function genetic screens to elucidate the key mediators of OIS upon inhibition of TWIST1.

The requirement of TWIST1 for bypassing OIS appears to extend across multiple driver oncogenes. Interestingly, a previous study had correlated increase *TWIST1* expression with the presence of *EGFR*-activating mutations (41). A follow-up study found that TWIST1 may play a role in migration and EGF-mediated EMT in a limited subset of EGFR-mutant cell lines in short-term experiments (42). In our present study, we show a critical requirement for TWIST1 in *EGFR*-mutant NSCLCs in long-term growth experiments *in vitro* as well as *in vivo*.

Little is known about the requirement for *TWIST1* in *c-Met*–dependent NSCLCs. Interestingly, a recent report, has suggested that either pharmacologic inhibition of *c-Met* or silencing of *TWIST1* could inhibit metastasis in an *in vivo* breast cancer model by preventing EMT (43). We report for the first time that TWIST1 expression is essential for *c-Met*–dependent NSCLCs. The *c-Met* oncogene is amplified, mutated, and/or overexpressed in significant number of patients with NSCLCs. Furthermore, there is evidence of significant crosstalk and interdependence between the EGFR and c-Met signaling pathways (44). c-Met amplification is a recognized acquired resistance mechanism in patients treated with EGFR-targeted tyrosine kinase inhibitor (TKI; ref. 45). Multiple antibody-based and TKI-based therapies for targeting the c-Met pathway are currently in clinical trials for NSCLCs (44). Therefore, targeting *TWIST1* in *c-Met*–dependent NSCLCs represents a novel and promising therapeutic strategy.

Published OnlineFirst January 30, 2013; DOI: 10.1158/1541-7786.MCR-12-0456

In summary, our data suggest that TWIST1 represents an attractive therapeutic target for oncogene-driven NSCLCs. Inhibition of TWIST1 resulted in OIS and growth inhibition in diverse genetic backgrounds and was effective for 3 major classes of driver mutations in adenocarcinoma of the lung (*KRAS*-mutant, *EGFR*-mutant, and *c-Met*–amplified). While prenatal *TWIST1* haploinsufficiency leads to Saethre–Chotzen syndrome (23, 24), the expression of *TWIST1* is quite restricted postnatally, and some studies have even suggested that postnatal deletion of this loci may be well-tolerated (46, 47). To this end, we are currently developing a cell-based assay to screen for small molecules that may inhibit TWIST1 transcriptional activity.

Disclosure of Potential Conflicts of Interest

Y.-J. Cho has Honoraria from Speakers Bureau of Novartis and is a consultant/advisory board member of Novartis. C.M. Rudin is a consultant/advisory board member of Eli Lilly. No potential conflicts of interest were disclosed by the other authors.

Authors' Contributions

Conception and design: T.F. Burns, P.T. Tran, C.M. Rudin
Development of methodology: T.F. Burns
Acquisition of data (provided animals, acquired and managed patients, provided facilities, etc.): T.F. Burns, I. Dobromilskaya, R.P. Gajula, S. Thiyagarajan, S.N.H. Chatley
Analysis and interpretation of data (e.g., statistical analysis, biostatistics, computational analysis): T.F. Burns, S. Thiyagarajan, S.N.H. Chatley, Y.-J. Cho, P.T. Tran, C.M. Rudin
Writing, review, and/or revision of the manuscript: T.F. Burns, Y.-J. Cho, P.T. Tran, C.M. Rudin
Administrative, technical, or material support (i.e., reporting or organizing data, constructing databases): T.F. Burns, S.C. Murphy, K. Aziz, P.T. Tran
Study supervision: T.F. Burns, P.T. Tran, C.M. Rudin

Acknowledgments

The authors thank members of the Rudin, Burns, Tran, and Hann laboratories for discussion and advice regarding this work.

Grant Support

This research was supported by the Flight Attendant Medical Research Institute, the Burroughs Wellcome Fund (C.M. Rudin), the 2010 AACR-AstraZeneca Fellowship for Translational Lung Cancer Research, 2010 ASCO Young Investigator Award and an Institutional T32 grant "Molecular Targets for Cancer Detection and Treatment" (T.F. Burns), and a Parker B. Francis Fellowship, an ACS Scholar award (122688-RSG-12-196-01-TBG), Uniting Against Lung Cancer Award and ASTRO Junior Faculty Research Training Award (to P.T. Tran).

The costs of publication of this article were defrayed in part by the payment of page charges. This article must therefore be hereby marked *advertisement* in accordance with 18 U.S.C. Section 1734 solely to indicate this fact.

Received July 25, 2012; revised December 12, 2012; accepted December 30, 2012; published OnlineFirst January 30, 2013.

References

1. Siegel R, Ward E, Brawley O, Jemal A. Cancer statistics, 2011: the impact of eliminating socioeconomic and racial disparities on premature cancer deaths. CA Cancer J Clin 2011;61:212–36.
2. Mok TS. Personalized medicine in lung cancer: what we need to know. Nat Rev Clin Oncol 2011;8:661–8.
3. Sequist LV, Waltman BA, Dias-Santagata D, Digumarthy S, Turke AB, Fidias P, et al. Genotypic and histological evolution of lung cancers acquiring resistance to EGFR inhibitors. Sci Transl Med 2011;3:75ra26.
4. Katayama R, Shaw AT, Khan TM, Mino-Kenudson M, Solomon BJ, Halmos B, et al. Mechanisms of acquired crizotinib resistance in ALK-rearranged lung cancers. Sci Transl Med 2012;4:120ra17.
5. Riely GJ, Marks J, Pao W. KRAS mutations in non-small cell lung cancer. Proc Am Thorac Soc 2009;6:201–5.
6. Luo J, Solimini NL, Elledge SJ. Principles of cancer therapy: oncogene and non-oncogene addiction. Cell 2009;136:823–37.
7. Barbie DA, Tamayo P, Boehm JS, Kim SY, Moody SE, Dunn IF, et al. Systematic RNA interference reveals that oncogenic KRAS-driven cancers require TBK1. Nature 2009;462:108–12.
8. Luo J, Emanuele MJ, Li D, Creighton CJ, Schlabach MR, Westbrook TF, et al. A genome-wide RNAi screen identifies multiple synthetic lethal interactions with the Ras oncogene. Cell 2009;137:835–48.
9. Puyol M. A synthetic lethal interaction between K-Ras oncogenes and Cdk4 unveils a therapeutic strategy for non-small cell lung carcinoma. Cancer Cell 2010;18:63–73.
10. Scholl C, Fröhling S, Dunn IF, Schinzel AC, Barbie DA, Kim SY, et al. Synthetic Lethal interaction between oncogenic KRAS dependency and STK33 suppression in human cancer cells. Cell 2009;137:821–34.
11. Singh A, Greninger P, Rhodes D, Koopman L, Violette S, Bardeesy N, et al. A Gene expression signature associated with "K-Ras Addiction" reveals regulators of EMT and tumor cell survival. Cancer Cell 2009;15:489–500.
12. Babij C, Zhang Y, Kurzeja RJ, Munzli A, Shehabeldin A, Fernando M, et al. STK33 kinase activity is non-essential in KRAS-dependent cancer cells. Cancer Res 2011;71:5818–26.
13. Collado M, Serrano M. Senescence in tumours: evidence from mice and humans. Nat Rev Cancer 2010;10:51–7.
14. Acosta JC, Gil J. Senescence: a new weapon for cancer therapy. Trends Cell Biol 2012;22:211–9.
15. Nardella C, Clohessy JG, Alimonti A, Pandolfi PP. Pro-senescence therapy for cancer treatment. Nat Rev Cancer 2011;11:503–11.
16. Collado M. Tumour biology: senescence in premalignant tumours. Nature 2005;436:642.
17. Prieur A, Peeper DS. Cellular senescence in vivo: a barrier to tumorigenesis. Curr Opin Cell Biol 2008;20:150–5.
18. Serrano M, Lin AW, McCurrach ME, Beach D, Lowe SW. Oncogenic ras provokes premature cell senescence associated with accumulation of p53 and p16INK4a. Cell 1997;88:593–602.
19. Lin HK. Skp2 targeting suppresses tumorigenesis by Arf-p53-independent cellular senescence. Nature 2010;464:374–9.
20. Ansieau S, Bastid J, Doreau A, Morel AP, Bouchet BP, Thomas C, et al. Induction of EMT by twist proteins as a collateral effect of tumor-promoting inactivation of premature senescence. Cancer Cell 2008;14:79–89.
21. Lee KE, Bar-Sagi D. Oncogenic KRas suppresses inflammation-associated senescence of pancreatic ductal cells. Cancer Cell 2010;18:448–58.
22. Barnes RM, Firulli AB. A twist of insight - the role of Twist-family bHLH factors in development. Int J Dev Biol 2009;53:909–24.
23. Chen ZF, Behringer RR. twist is required in head mesenchyme for cranial neural tube morphogenesis. Genes Dev 1995;9:686–99.
24. el Ghouzzi V, Le Merrer M, Perrin-Schmitt F, Lajeunie E, Benit P, Renier D, et al. Mutations of the TWIST gene in the Saethre-Chotzen syndrome. Nat Genet 1997;15:42–6.
25. Ansieau S, Morel AP, Hinkal G, Bastid J, Puisieux A. TWISTing an embryonic transcription factor into an oncoprotein. Oncogene 2010;29:3173–84.
26. Tran PT, Shroff EH, Burns TF, Thiyagarajan S, Das ST, Zabuawala T, et al. Twist1 suppresses senescence programs and thereby accelerates and maintains mutant Kras-induced lung tumorigenesis. PLoS Genet 2012;8:e1002650.
27. Ozoren N, Fisher MJ, Kim K, Liu CX, Genin A, Shifman Y, et al. Homozygous deletion of the death receptor DR4 gene in a nasopharyngeal cancer cell line is associated with TRAIL resistance. Int J Oncol 2000;16:917–25.

Published OnlineFirst January 30, 2013; DOI: 10.1158/1541-7786.MCR-12-0456

28. Moffat J, Grueneberg DA, Yang X, Kim SY, Kloepfer AM, Hinkle G, et al. A lentiviral RNAi library for human and mouse genes applied to an arrayed viral high-content screen. Cell 2006;124:1283–98.
29. Sarbassov DD, Guertin DA, Ali SM, Sabatini DM. Phosphorylation and regulation of Akt/PKB by the rictor-mTOR complex. Science 2005;307:1098–101.
30. Wiederschain D, Wee S, Chen L, Loo A, Yang G, Huang A, et al. Single-vector inducible lentiviral RNAi system for oncology target validation. Cell Cycle 2009;8:498–504.
31. Maestro R, Dei Tos AP, Hamamori Y, Krasnokutsky S, Sartorelli V, Kedes L, et al. Twist is a potential oncogene that inhibits apoptosis. Genes Dev 1999;13:2207–17.
32. Serres MP, Zlotek-Zlotkiewicz E, Concha C, Gurian-West M, Daburon V, Roberts JM, et al. Cytoplasmic p27 is oncogenic and cooperates with Ras both in vivo and in vitro. Oncogene 2011;30:2846–58.
33. Wander SA, Zhao D, Slingerland JM. p27: a barometer of signaling deregulation and potential predictor of response to targeted therapies. Clin Cancer Res 2011;17:12–8.
34. Frescas D, Pagano M. Deregulated proteolysis by the F-box proteins SKP2 and beta-TrCP: tipping the scales of cancer. Nat Rev Cancer 2008;8:438–49.
35. Subramanian A, Tamayo P, Mootha VK, Mukherjee S, Ebert BL, Gillette MA, et al. Gene set enrichment analysis: a knowledge-based approach for interpreting genome-wide expression profiles. Proc Natl Acad Sci U S A 2005;102:15545–50.
36. Shiota M, Izumi H, Onitsuka T, Miyamoto N, Kashiwagi E, Kidani A, et al. Twist promotes tumor cell growth through YB-1 expression. Cancer Res 2008;68:98–105.
37. Piccinin S, Tonin E, Sessa S, Demontis S, Rossi S, Pecciarini L, et al. A "twist box" code of p53 inactivation: twist box: p53 interaction promotes p53 degradation. Cancer Cell 2012;22:404–15.
38. Shiota M, Izumi H, Onitsuka T, Miyamoto N, Kashiwagi E, Kidani A, et al. Twist and p53 reciprocally regulate target genes via direct interaction. Oncogene 2008;27:5543–53.
39. Vichalkovski A, Gresko E, Hess D, Restuccia DF, Hemmings BA. PKB/AKT phosphorylation of the transcription factor Twist-1 at Ser42 inhibits p53 activity in response to DNA damage. Oncogene 2010;29:3554–65.
40. Xu M. Beta-catenin expression results in p53-independent DNA damage and oncogene-induced senescence in prelymphomagenic thymocytes *in vivo*. Mol Cell Biol 2008;28:1713–23.
41. Blons H, Pallier K, Le Corre D, Danel C, Tremblay-Gravel M, Houdayer C, et al. Genome wide SNP comparative analysis between EGFR and KRAS mutated NSCLC and characterization of two models of oncogenic cooperation in non-small cell lung carcinoma. BMC Med Genomics 2008;1:25.
42. Pallier K, Cessot A, Cote JF, Just PA, Cazes A, Fabre E, et al. TWIST1 a new determinant of epithelial to mesenchymal transition in EGFR mutated lung adenocarcinoma. PloS One 2012;7:e29954.
43. Cooke Vesselina G, LeBleu Valerie S, Keskin D, Khan Z, O'Connell Joyce T, Teng Y, et al. Pericyte depletion results in hypoxia-associated epithelial-to-mesenchymal transition and metastasis mediated by Met signaling pathway. Cancer Cell 2012;21:66–81.
44. Feng Y, Thiagarajan PS, Ma PC. MET signaling: novel targeted inhibition and its clinical development in lung cancer. J Thorac Oncol 2012;7:459–67.
45. Oxnard GR, Arcila ME, Chmielecki J, Ladanyi M, Miller VA, Pao W. New strategies in overcoming acquired resistance to epidermal growth factor receptor tyrosine kinase inhibitors in lung cancer. Clin Cancer Res 2011;17:5530–7.
46. Chen YT, Akinwunmi PO, Deng JM, Tam OH, Behringer RR. Generation of a Twist1 conditional null allele in the mouse. Genesis 2007;45:588–92.
47. Pan D, Fujimoto M, Lopes A, Wang YX. Twist-1 is a PPARdelta-inducible, negative-feedback regulator of PGC-1alpha in brown fat metabolism. Cell 2009;137:73–86.

Supplemental Table 1: Mutational status of cell lines studied

Cell line	Histology	KRAS mutation[a]	p53 status	p16 status	Additional mutations[a]	Mechanism
A549	AC	p.G12S	wild type[a]	deletion[a]		senescence/arrest
H358	AC	p.G12C	deletion[b]	meth[b]		senescence/arrest
H23	AC	p.G12C	Pl.M246.I	meth[b]		senescence/arrest
H460	LC	p.Q61H	wild type	deletion[a]	PIK3CA (p.E545K) GA-Myc	senescence/arrest
H727	Carcinoid	p.G12V	insertion[a]	meth[b]		senescence/arrest
Calu-1	SCC	p.G12C	deletion[d]	meth[e]		apoptosis
Calu-6	Anaplastic carcinoma	p.Q61K	p.R196X[a]	meth[e]		apoptosis
H1975	AC	wild type	p.R273H[a]	E69*[a]	EGFR (L858R, T790M) PIK3CA (pG118D)	arrest
H3255	AC	wild type[f]	intron 5[g]	deletion	EGFR (L858R)[f]	arrest
H1993	AC	wild type	p.242W	deletion	c-Met amplified	Arrest

a – The data was obtained from the Wellcome Trust Sanger Institute Cancer Genome Project web site, http://www.sanger.ac.uk/genetics/CGP, accessed June 19, 2012
b – (1)
c – (2)
d – The data was obtained from the UMD p53 mutation database, http://p53.free.fr/index.html, accessed June 19, 2012
e – (3)
f – (4)
g – (5)

Supplemental Figure Legends

Supplemental Figure 1. TWIST1 specific shRNAs suppress *TWIST1* transcript and protein levels. **A.** The shRNAs shTWIST1-1 and shTWIST1-2 suppress *TWIST1* transcript levels as shown by qPCR at day 4 after the shRNA infection in the indicated cell lines. **B.** *TWIST1* specific shRNAs suppress TWIST1 protein expression as shown by western blot analysis at day 6 after shRNA infection in H460 and A549 cells. shTWIST1-1 (shTWIST1-39) and shTWIST1-2 (shTWIST1-43) were used for all further studies.

Supplemental Figure 2. Mouse *Twist1* can rescue the anti-proliferative effects of knockdown of human *TWIST1* in A549 cells. **A.** Twist1 Western blot of A549 cells stably infected with mouse *Twist1*. **B.** Mouse *Twist1* rescues the anti-proliferative phenotype of human *TWIST1* knockdown in A549 cells as shown by crystal violet staining of cells in triplicate

Supplemental Figure 3. Growth inhibition by silencing *TWIST1* is not p53-dependent in *KRAS* mutant NSCLC. **A.** *TP53* knockdown in H460 and A549 cells prevents induction of p53 and its target gene, p21 after *TWIST1* knockdown as shown by Western blotting on day 4 after the shRNA infection. **B.** Representative triplicates of crystal violet staining of H460 or A549 NSCLC cells demonstrate *TWIST1* knockdown with 2 separate shRNAs decreases cellular proliferation despite the absence of p53.

Supplemental Figure 4. Growth inhibition by silencing *TWIST1* is not p21-dependent in *KRAS* mutant NSCLC. **A.** p21 knockdown inhibits p21 induction after *TWIST1* knockdown in H460, A549, and H727 lines as shown by Western blotting on day 4. **B.** Representative triplicates of crystal violet staining in all lines after *TWIST1* knockdown with 2 separate shRNAs decreases cellular proliferation despite suppression of p21.

Supplemental Figure 5. Growth inhibition by silencing TWIST1 is not dependent on induction of p27 in KRAS mutant NSCLC **A.** p27 knockdown with 2 separate shRNAs in H460 prevents induction of p27 after TWIST1 knockdown as shown by Western blotting on day 6 after shRNA infection. **B.** Representative triplicates of crystal violet staining in H460 cells demonstrate that TWIST1 knockdown decreased cellular proliferation despite the absence of p27.

Supplemental Figure 6. Overexpression of *SKP2* does not rescue loss of *TWIST1* in *KRAS* mutant NSCLC. **A.** Overexpression of exogenous SKP2 in H460 and A549 cells decreases the protein levels of p27 as shown by Western blotting on day 6 after shRNA infection. **B.** Representative triplicates of crystal violet staining in H460 and A549 cells demonstrate that *TWIST1* knockdown with 2 separate shRNAs decreases cellular proliferation despite the overexpression of SKP2.

Supplemental Figure 7. Microarray analysis of three *KRAS* mutant NSCLC cell lines (H460, H727 and H358) six days after silencing of *TWIST1* reveals a striking cell cycle arrest gene signature. Heat maps of top 75 ranked genes that decreased (left) or increased (right) after *TWIST1* knockdown.

Supplemental Figure 8. Enrichment plots after Gene Set Enrichment Analysis for **A.** ROSTY_CERVICAL_CANCER_PROLIFERATION_CLUSTER (left) CROONQUIST_IL6_DEPRIVATION_DN (middle) CHANG_CYCLING_GENES (right) **B.** KANG_DOXORUBICIN_RESISTANCE_UP **C.** BLUM_RESPONSE_TO_SALIRASIB DN (left) CROONQUIST_NRAS_SIGNALING_DN (right) **D.** FUJII_YBX1_TARGETS_DN following GSEA performed on shScram and shTWIST1 samples from three *KRAS* mutant cell lines (H460, H727 and H358) six days after *TWIST1* knockdown samples (NOM *p*-values, FDR *q*-values, and FWER *p*-values were all <0.001 for all gene sets).

Supplemental materials and methods

SYBER-green quantitative RT-PCR

Total RNA was isolated from tissue using the Qiaprep RNAeasy Kit (Qiagen) according to the manufacturer's directions. Samples were treated with RQ1 RNase-Free DNase (Promega). cDNA was generated from 1 µg of total RNA using the Superscript II kit (Invitrogen Technologies). Control reactions were run without RT enzyme (Perkin Elmer). 50 ng of cDNA equivalents were amplified for the transcript described below in an ABI-prism 7700 (Perkin Elmer Applied Biosystems) for 40 cycles using SYBR green PCR Master mix (Perkin Elmer Applied Biosystems) according to manufacturer's directions. PCR reactions were performed in duplicate-triplicate in a final volume of 20 µL. Following amplification, the data was processed with the analysis program Sequence Detection Systems v2.2.2 (Applied Biosystems). For each sample, the level of RNA for the genes of interest was standardized to a housekeeping gene (ubiquitin or 18S rRNA) within that sample; subsequently, the level of a transcript of interest was normalized to the expression of that transcript from the appropriate comparator sample. PCR primer were used as previously described (6).

Microarray Analysis and Gene Set Enrichment Analysis

Total RNA was isolated as described for qPCR, applied to Illumina arrays, files preprocessed and normalized using default parameters in the Genespring GX 11 software package (Agilent, Santa Clara, CA) or the DASL pipeline in Genepattern (www.broadinstitute.org/genepattern). Arrays were visualized using Genespring GX 11 or GenePattern software packages. Gene set enrichment analysis (GSEA) was performed as previously described (7) using a reference database of 2,163 gene sets: 1,891 gene sets from the MSigDB-C2 database [http://www.broad.mit.edu/gsea/msigdb] and 272 additional manually curated gene sets representing oncogene activation/tumor suppressor deregulation (OPAM database v3) (8). To all gene sets we added sets that combined up and down regulated sets derived from the same experimental condition or publication. The final total was 2,599 signatures. For 'single sample' gene set enrichment analysis (ssGSEA) we define a numerical score to represent the single-sample absolute enrichment in each of the samples for each of gene set of interest using the following procedure. Probes in each pre-processed gene-expression dataset were mapped to gene symbols using the probe "collapse" feature from GSEA analysis [www.broad.mit.edu/gsea] and the genes ranked by absolute expression for each sample. The enrichment score is produced by evaluating a weighted integral (sum) of the difference between the Empirical

Cumulative Distribution Functions (ECDF) of the genes in the gene set vs. genes not in the set, rather than the maximum (Kolmogorov- Smirnov) as used in GSEA. For gene sets with up-regulated (UP) and down-regulated (DN) versions, a combined score is produced by adding the UP and DN scores (with negative sign). To quantify the degree of matching between phenotypes vs. pathway profiles we used the area under the ROC (Receiver Operating Characteristic) curve ranging from 0.5 (random match) to 1.0 (perfect match). The statistical significance is computed using a binomial test. Both computations use the R "verification" package.

Immunoblot analysis.

The following primary antibodies was used: rabbit anti- Skp2 p45 (H-435, Santa Cruz) and mouse anti-Twist1 (TWIST2C1a, Santa Cruz).

Lentiviral shRNA and cDNA Overexpression Experiments.

The following shRNA constructs were obtained from the Broad RNAi Consortium and clone IDs as are follows: p21: TRCN0000040123 (shp21-1) and TRCN0000010401 (shp21-2) p27:: TRCN0000039932 and TRCN0000009857 and TWIST1: TRCN0000020540 (shTWIST1-40. pLKO.1-shRNA scramble vector was obtained from Dr. David M. Sabatini through Addgene (Addgene plasmid 1864) as previously described (9). The Tet-pLKO-puro vector was from Dmitri Wiederschain through Addgene (Addgene plasmid 21915) as previously described (10). The pLKO.1 – Neo vector was obtained from Sheila Stewart through Addgene (Addgene plasmid 13425) and oligonucleotides for TWIST1-1, TWIST1-2 and scrambled control were cloned into this vector and used to for experiments with shRNAs targeting p53, p21, p27 and overexpression of Skp2. The pLenti CMV Puro DEST (w118-1) vector was obtained from Eric Campeau through Addgene (Addgene plasmid 17452) (11). The Ultimate™ ORF (Invitrogen) for Skp2 (IOH 41200) was obtained from the Johns Hopkins University HiT Center and a LR reaction (Invitrogen) was performed to construct pLenti Puro DEST (w118-1)-Skp2. All constructs were sequence verified. Twenty-four hours after infection, cells were treated with 1 mg/ml puromycin or 500 mg/ml G418 and passaged once 80% confluent. Retroviral infections on A549 cells used pWZL-Hygro vector and pWZL-Hygro/mTwist1 constructs, for two successive times over a 36-h period and then followed by selection with hygromycin (250μg/ml) for 4 day as previously describe(6).

Supplemental references

1. Blanco R, Iwakawa R, Tang M, Kohno T, Angulo B, Pio R, et al. A gene-alteration profile of human lung cancer cell lines. Hum Mutat. 2009;30:1199-206.
2. Phelps RM, Johnson BE, Ihde DC, Gazdar AF, Carbone DP, McClintock PR, et al. NCI-Navy Medical Oncology Branch cell line data base. J Cell Biochem Suppl. 1996;24:32-91.
3. Shapiro GI, Park JE, Edwards CD, Mao L, Merlo A, Sidransky D, et al. Multiple mechanisms of p16INK4A inactivation in non-small cell lung cancer cell lines. Cancer research. 1995;55:6200-9.
4. Tracy S, Mukohara T, Hansen M, Meyerson M, Johnson BE, Janne PA. Gefitinib induces apoptosis in the EGFRL858R non-small-cell lung cancer cell line H3255. Cancer research. 2004;64:7241-4.
5. Zhang W, Stabile LP, Keohavong P, Romkes M, Grandis JR, Traynor AM, et al. Mutation and polymorphism in the EGFR-TK domain associated with lung cancer. Journal of thoracic oncology : official publication of the International Association for the Study of Lung Cancer. 2006;1:635-47.
6. Tran PT, Shroff EH, Burns TF, Thiyagarajan S, Das ST, Zabuawala T, et al. Twist1 suppresses senescence programs and thereby accelerates and maintains mutant Kras-induced lung tumorigenesis. PLoS genetics. 2012;8:e1002650.
7. Subramanian A, Tamayo P, Mootha VK, Mukherjee S, Ebert BL, Gillette MA, et al. Gene set enrichment analysis: a knowledge-based approach for interpreting genome-wide expression profiles. Proc Natl Acad Sci U S A. 2005;102:15545-50.
8. Barbie DA, Tamayo P, Boehm JS, Kim SY, Moody SE, Dunn IF, et al. Systematic RNA interference reveals that oncogenic KRAS-driven cancers require TBK1. Nature. 2009;462:108-12.
9. Sarbassov DD, Guertin DA, Ali SM, Sabatini DM. Phosphorylation and regulation of Akt/PKB by the rictor-mTOR complex. Science. 2005;307:1098-101.
10. Wiederschain D, Wee S, Chen L, Loo A, Yang G, Huang A, et al. Single-vector inducible lentiviral RNAi system for oncology target validation. Cell Cycle. 2009;8:498-504.
11. Campeau E, Ruhl VE, Rodier F, Smith CL, Rahmberg BL, Fuss JO, et al. A versatile viral system for expression and depletion of proteins in mammalian cells. PLoS One. 2009;4:e6529.

Supplemental Figure 1

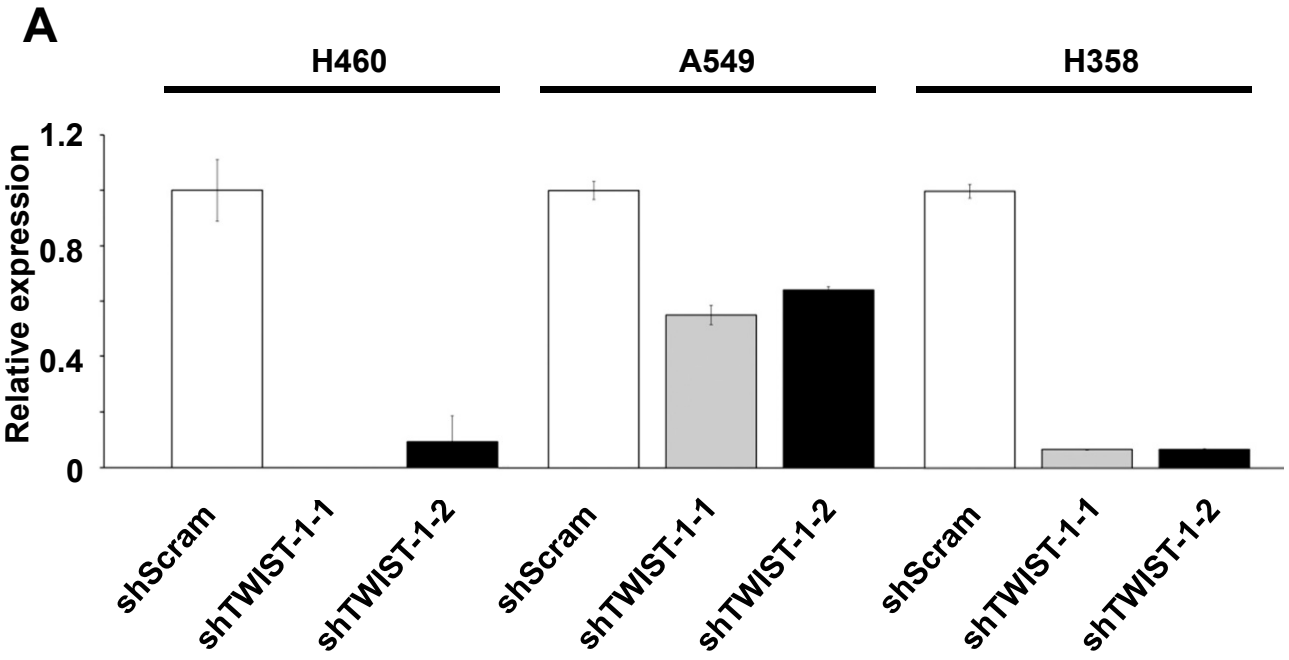

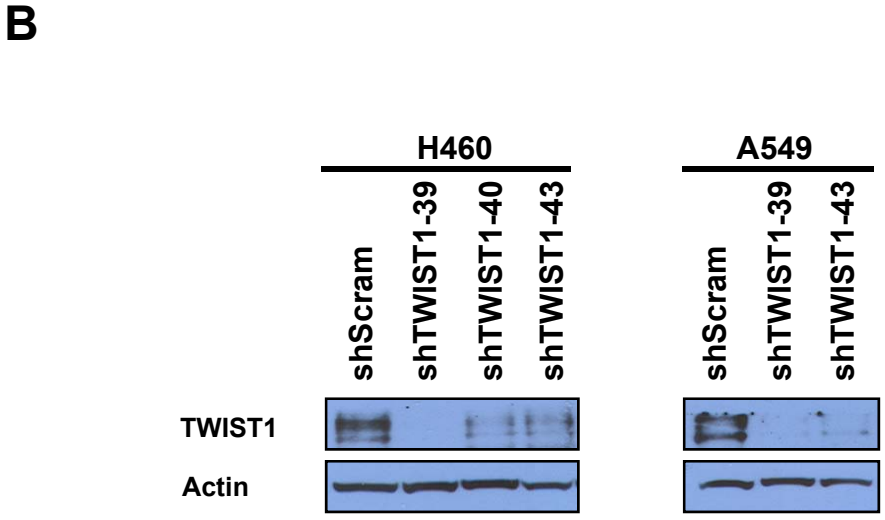

Supplemental Figure 2

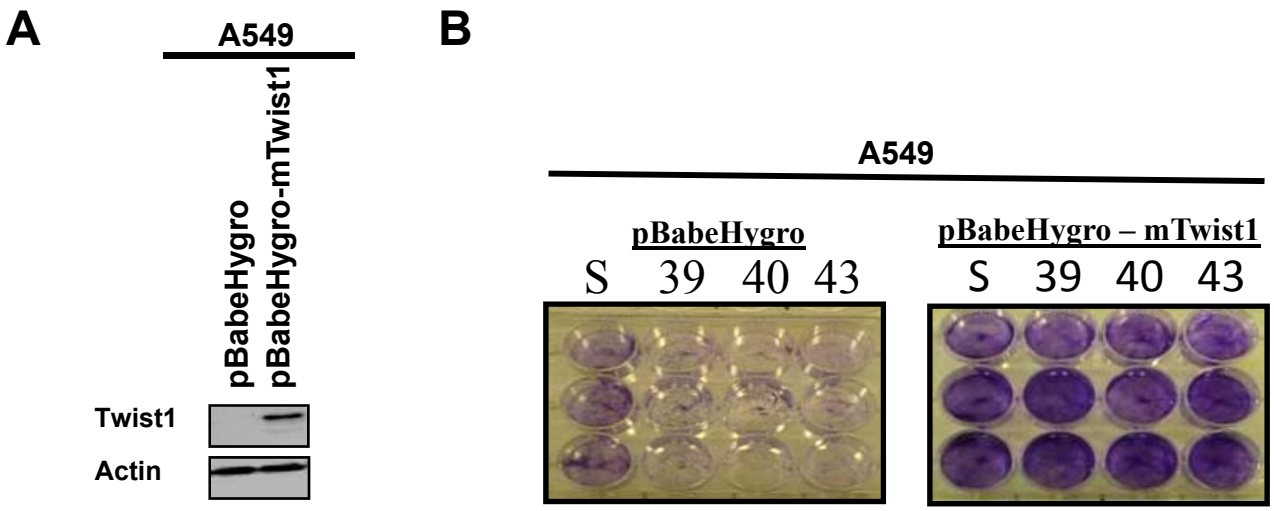

Supplemental Figure 3

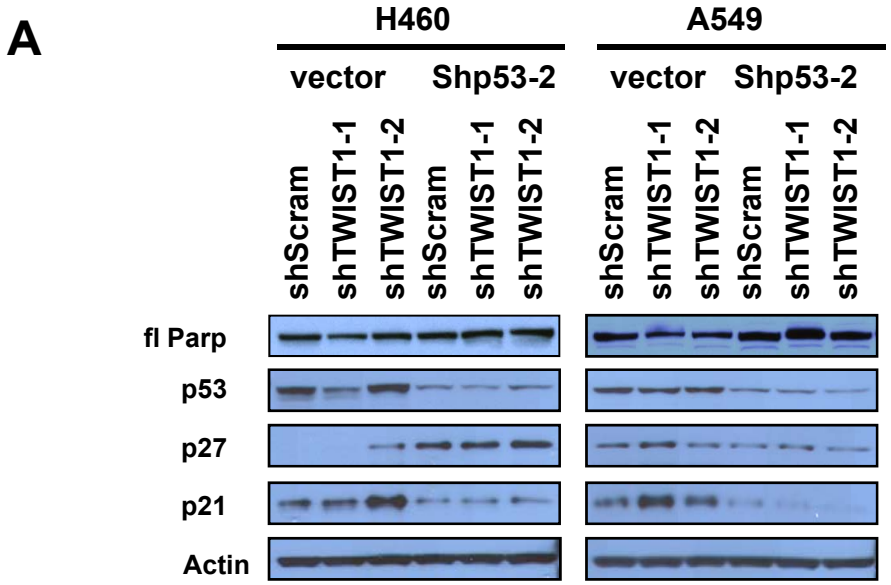

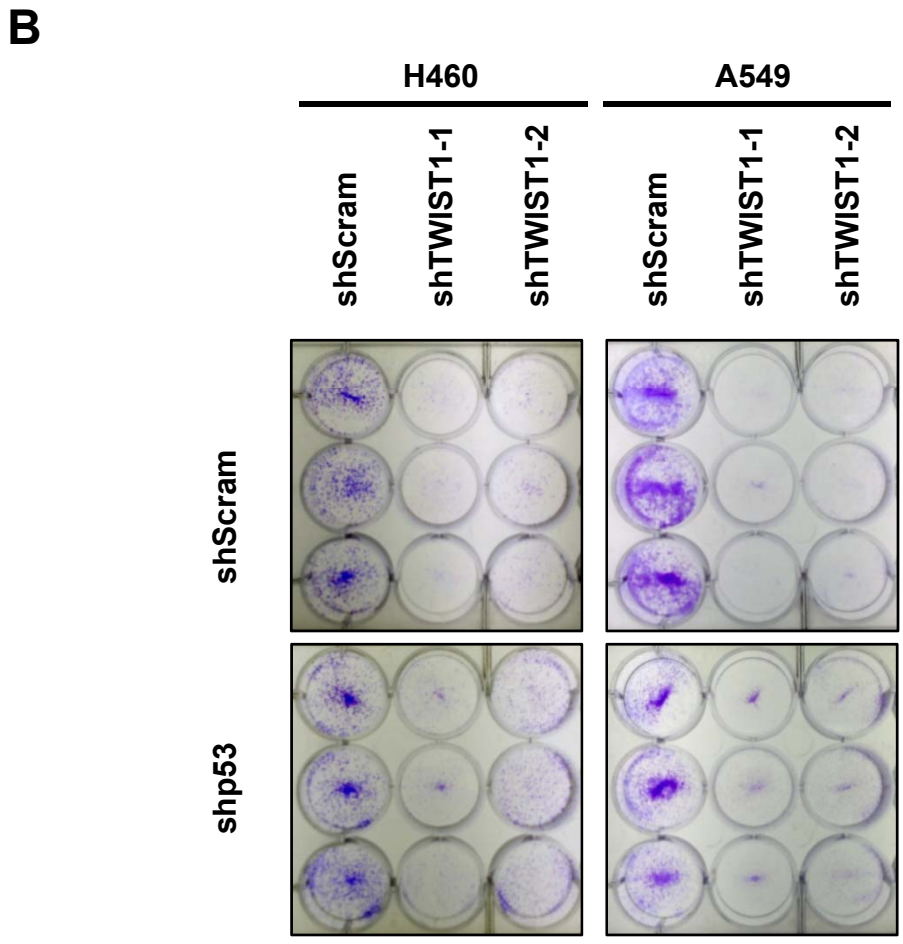

Supplemental Figure 4

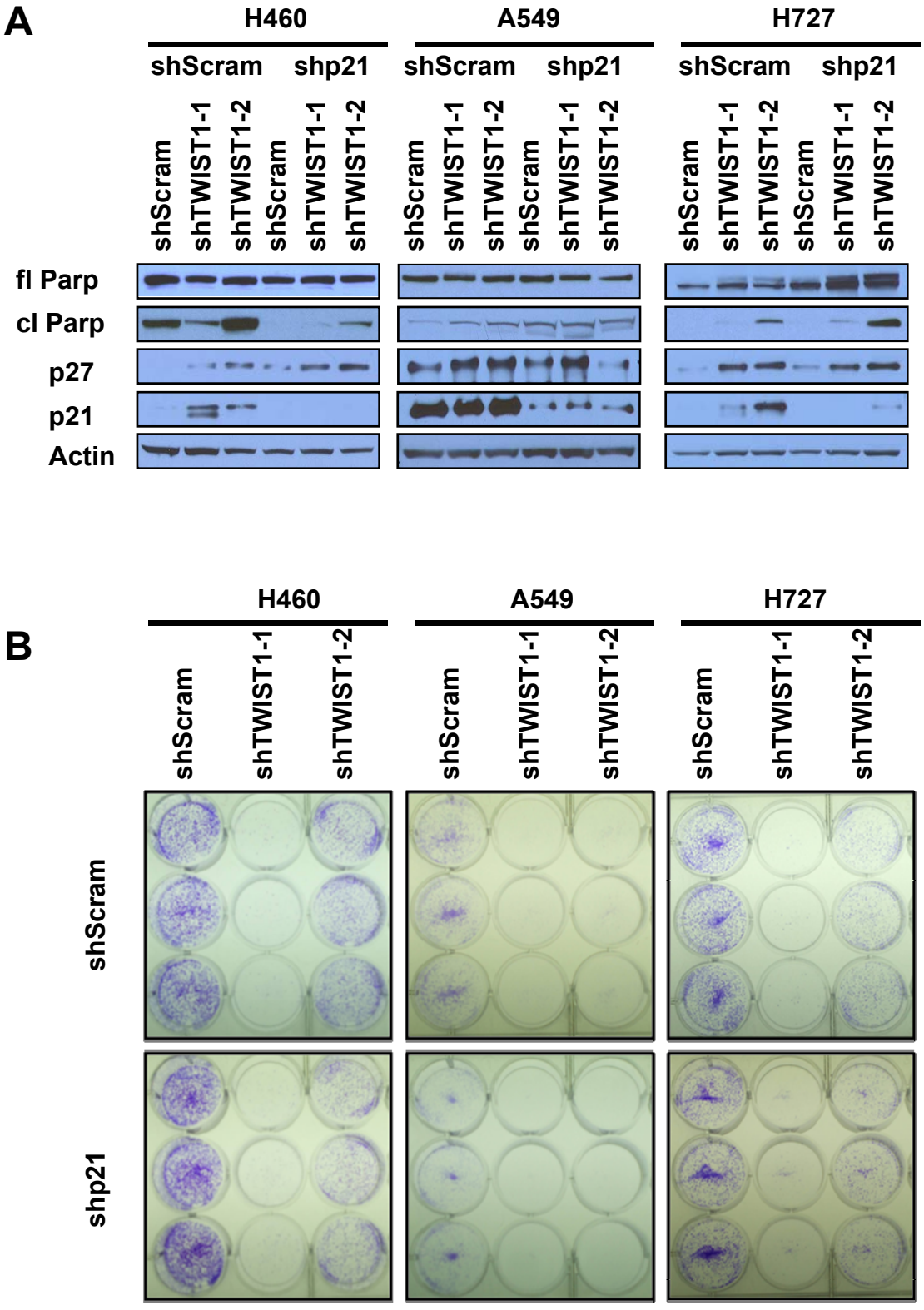

Supplemental Figure 5

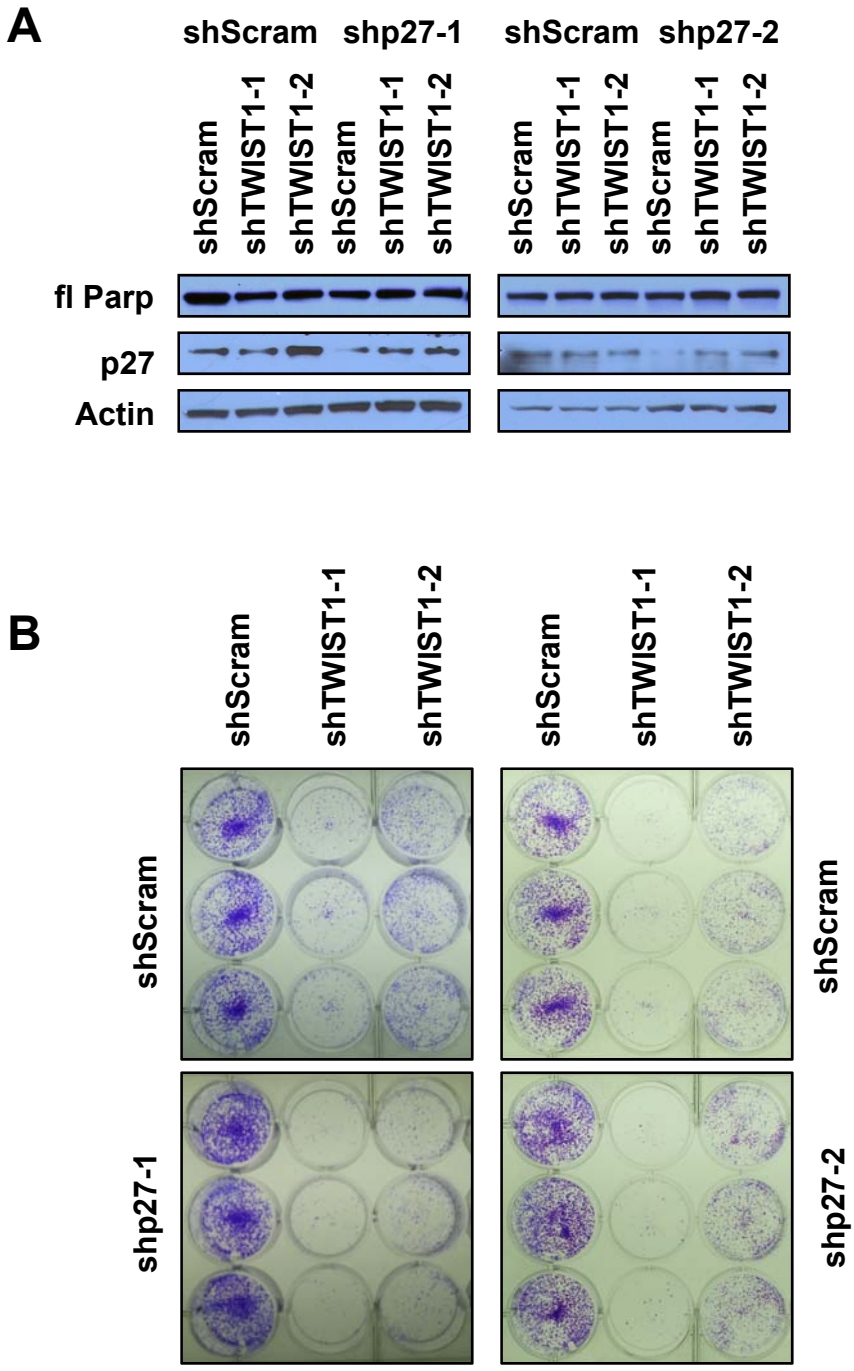

Supplemental Figure 6

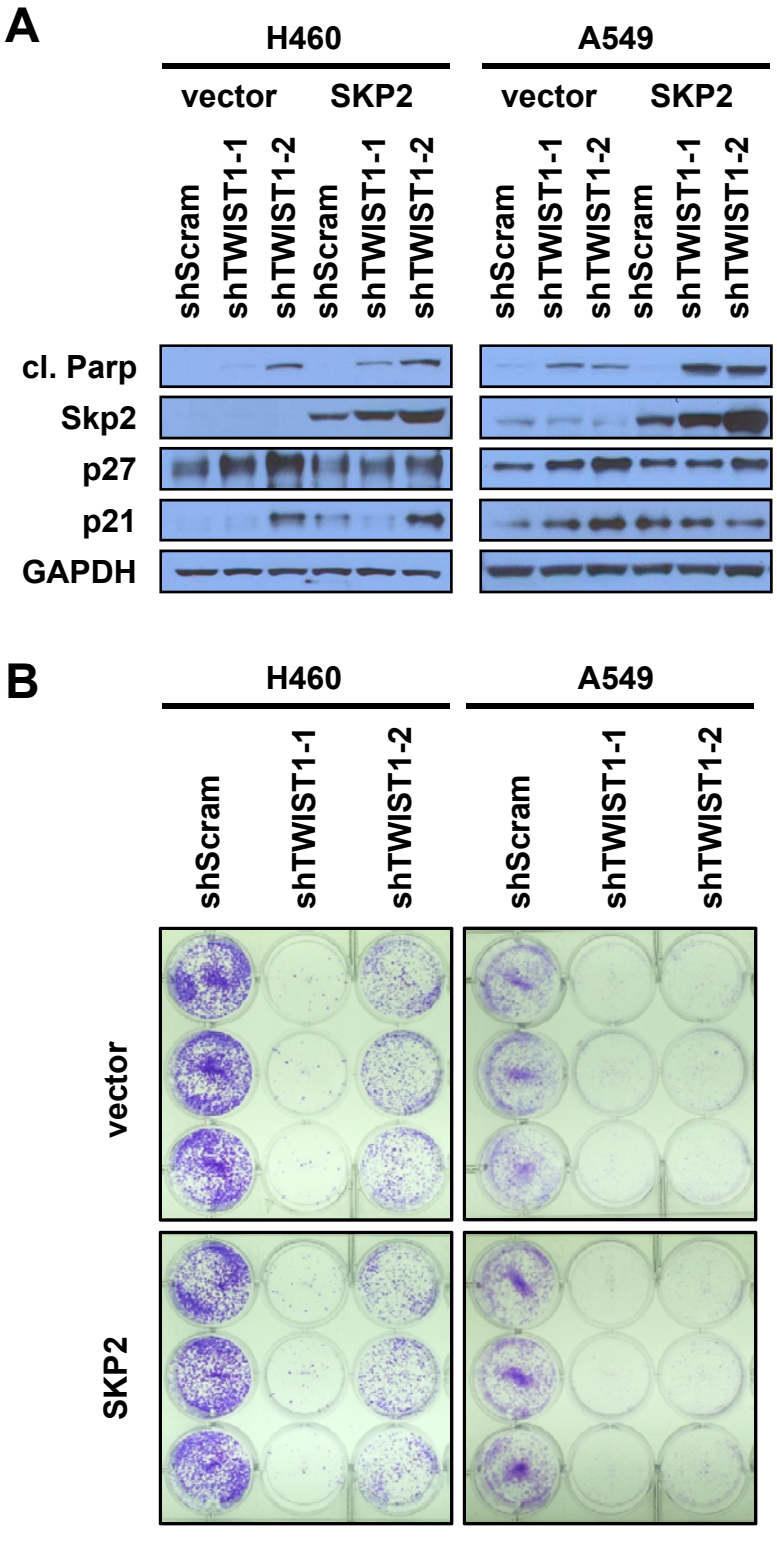

Supplemental Figure 7

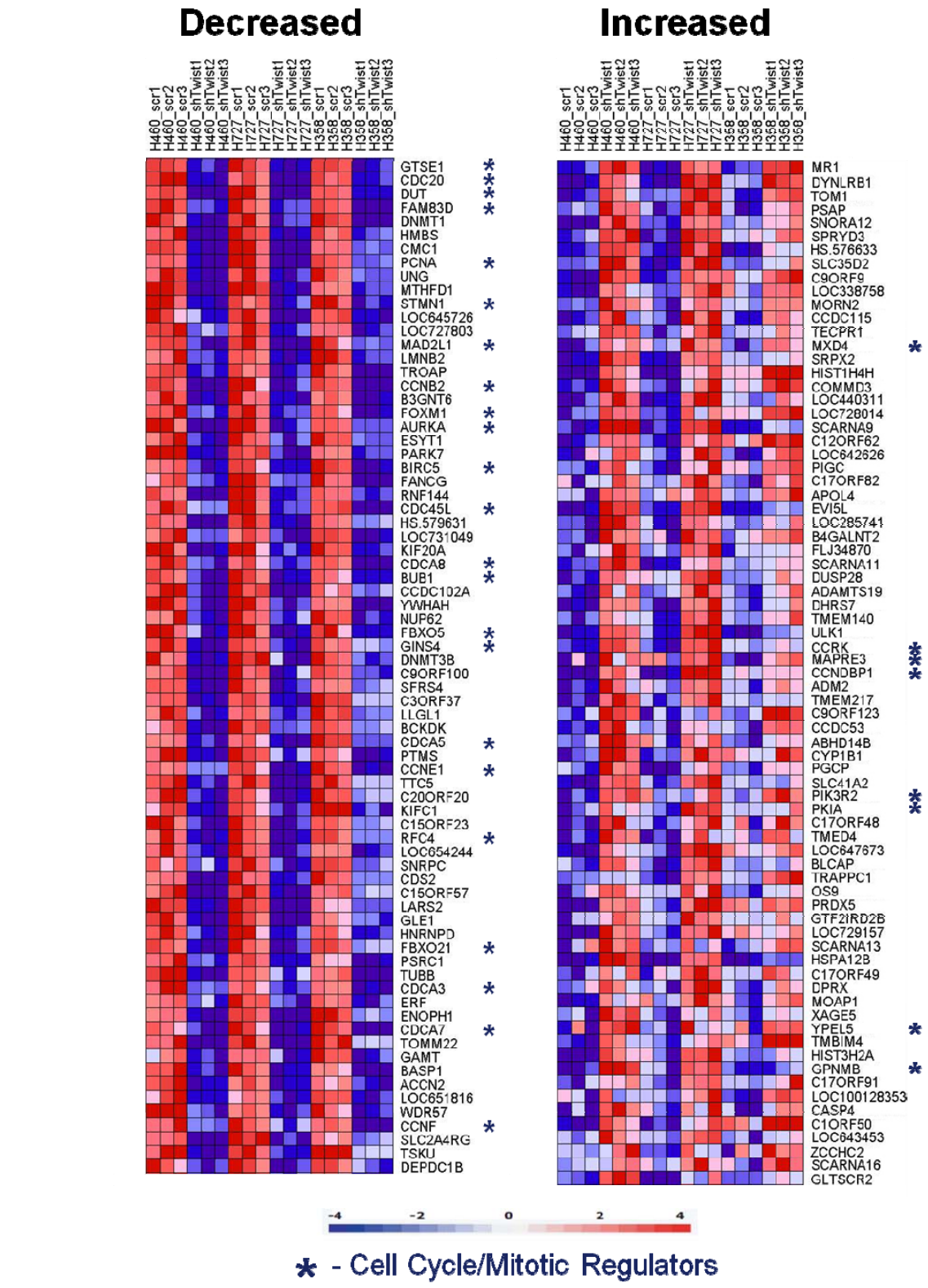

Supplemental Figure 8

A

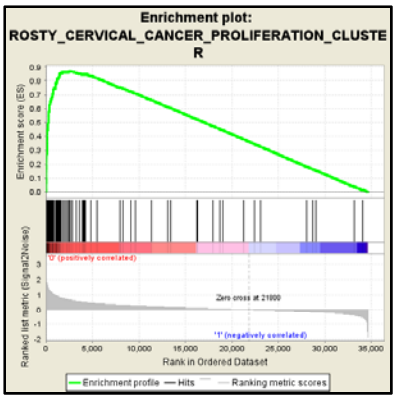

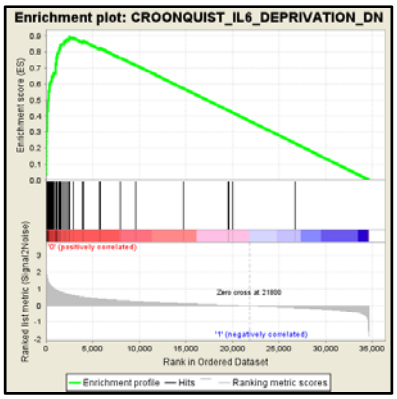

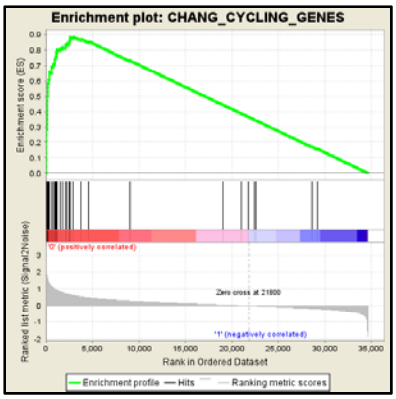

B

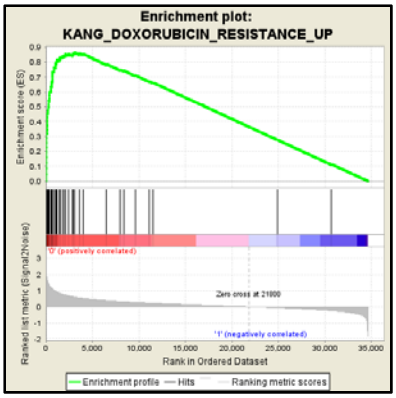

C

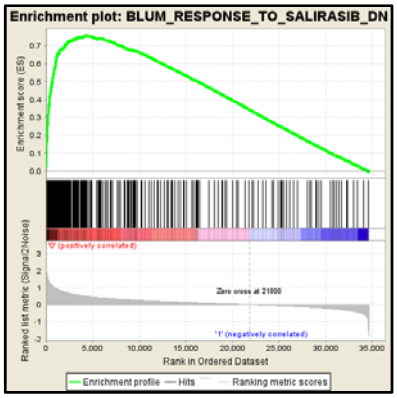

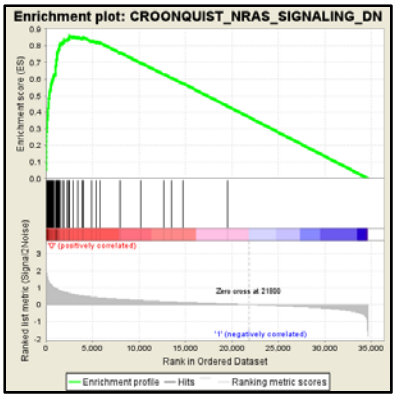

D